RAMAN SPECTRA AND PHOTOLUMINESCENCE OF POLYCRYSTALLINE $CaGa_2S_4:Tb^{3+}$ COMPOUND

E.F.GAMBAROV

Institute of Physics Azerbaijan Academy of Sciences,

H. Javid av. 33, Baku, 370143, Azerbaijan

Raman and photoluminescence studies of $CaGa_2S_4$ compound was performed. The orthorhombic thiogallate $CaGa_2S_4:Tb^{3+}$ exhibits phonon energies: 280 cm^{-1} (~35 meV) and 360 cm^{-1} (~45 meV) for the most intense vibration modes. Factor group model predicts that the total number of Raman-active phonons is 84 for this structure.
It is shown that the excitation spectra contains wide intense band (max~320 nm) and emission process of $CaGa_2S_4:Tb^{3+}$ connected with radiative ($^5D_4 \rightarrow {}^7F_6$, $^5D_4 \rightarrow {}^7F_5$, $^5D_4 \rightarrow {}^7F_4$, $^5D_4 \rightarrow {}^7F_3$) energy transitions of Tb^{3+} ions.
Decay characterisation of intensive maximum (545 nm) shows that the lifetime of Tb^{3+} ions is 2.7 ns (fast decay) and 615 μs (long decay).

1. Introduction

Ternary compounds of general formula $M^{II}M^{III}_2(S,Se)_4$ (where M^{II} and M^{III} are respectively divalent and trivalent cations) form an extensive class of semiconductors and present luminescent properties when doped with rare earth elements. Photoluminescence and cathodoluminescence properties of thiogallate compounds doped with rare earth activators have been studied since the seventies [1-5]. The Eu^{2+}- and Ce^{3+} doped CaGa2S4 and $SrGa_2S_4$ compounds are well known respectively as efficient green and blue phosphors with excellent colour coordinates [1]. They have been claimed as promising candidates for full-colour Thin Film Electroluminescence (TFEL) displays [6] and Field Emission Display (FED) applications [7]. The aim of this work is to clarify the origins of the vibration modes in the chalcogallate based phosphors in order to increase the knowledge about the lattice dynamical properties that influence the luminescence efficiency. Indeed, among the non-radiative transition mechanisms leading to a thermal relaxation of the luminescent centre, a multiphonon process is often observed between 4f excited levels of rare-earth ions. It involves mainly the high-energy optical phonons. The non-radiative multiphonon transition probability is increasing with the frequency increase of the high-energy phonons of the lattice. In the case of ElectroLuminescent (EL) materials, the most frequent scattering event under high electric field is the emission of optical phonons and the cooling of "hot electrons" is dominated by the coupling to the high-frequency modes. The scattering rate is lower for EL phosphors presenting low phonon energies. For CathodoLuminescent (CL) materials the rate of phonon energy loss is controlled by the phonons with highest energy and the CL efficiency of the phosphors decreases with increasing phonon energy [8]. This work is also an opportunity to collect spectra of powders $CaGa_2S_4:Tb^{3+}$ that will be used as references to study by Raman spectroscopy and photoluminescence the quality of thin films prepared for device applications.

2. Samples and experimental details

$CaGa_2S_4$ compound was obtained from an intimate mixture of CaS and Ga_2S_3 in a single zone furnace in quartz ampoules at 1200°C. The good crystalline properties of the powders were showed by XRD measurements .Activation by Tb (2 atom %) was realised using TbF_3 doping during the synthesis process.
The samples were excited by a pulsed nitrogen laser (Laser Photonics LN 1000, 1.4mJ energy per pulse, pulse width 0.6 ns). The emitted light from the sample, collected by an optical fiber located at 10mm perpendicular to the surface, was analysed with a Jobin-Yvon spectrometer HR460 and detector for visible range.
The decay curve was analyzed with a Jobin-Yvon HR360 monochromator coupled with: - a PM Hamamatsu R5600U and a scope Tektronix TDS 784A with a time constant of the order of 2 ns for the fast decay time; - a PM Hamamatsu R928 and a scope Nicolet 400 with a time constant of the order of 10 ns for the longer decay time. Stokes and anti-Stokes spectra were recorded between –500 cm^{-1} and +500 cm^{-1}. Line positions are determined by calculating the arithmetic average of both Stokes and anti-Stokes values. Raman scattering spectra of $CaGa_2S_4$ were measured by a Jobin-Yvon U1000 spectrometer with a Kr Spectrophysics laser and a photomultiplier counter at room temperature in back scattering configuration, with a laser excitation wavelength of λ= 676.4 nm and a laser power of 140 mW.

3. Results and discussion

3.1. Normal vibration modes

Stokes spectrum of the polycrystalline $CaGa_2S_4$ is given from 20 cm-1 to 500 cm-1 in fig.2. Each line in the Stokes part of the spectrum can be associated to an anti-stokes line positioned symmetrically with respect to the laser line frequency.

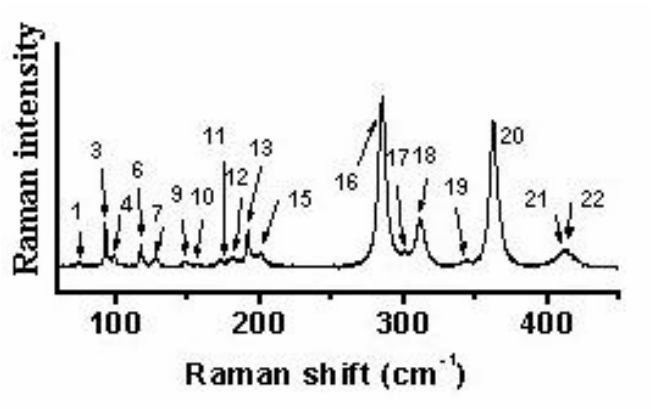

Fig.1. Raman spectra of polycrystalline $CaGa_2S_4$

The Stokes spectrum consists of 18 vibration lines positioned between ω=74.4 cm-1 and ω=413 cm-1 listed in table. In spectra the Raman vibration lines are divided into two groups separated by a domain without Raman frequencies between 200 and 275 cm^{-1}. Two intense vibration lines dominate the (Fig.1.) Raman spectra of polycrystalline $CaGa_2S_4$ 284.8-361.8 cm^{-1}.

Table.
X-Ray Diffraction data and Raman frequencies of polycrystalline $CaGa_2S_4:Tb^{3+}$

h	K	L	D(Å)	Raman frequencies(cm^{-1})
0	4	0	5.083	74.7
4	0	0		92.3
				98.3
2	2	2	4.624	117.2
				127.2
4	2	2	3.635	148.6
				156.5
0	6	2	2.934	171.8
				180.8
2	6	2	2.825	191.7
6	2	2		199.8
				284.8
0	8	0	2.533	300.8
8	0	0		311.4
2	4	4		342.5
				361.8
4	4	4	2.300	408.0
				413.0
4	8	0	2.251	
8	4	0		
5	7	5	1.682	
7	5	5		
3	9	5	1.593	
9	3	5		
12	2	2		

The $CaGa_2S_4$ compounds of the type $M^{II}Ga_2S_4$ (where M^{II}= Sr, Eu, Pb, Ca, Yb) belong to the orthorhombic crystal class with the space group D_{2h}^{24} (F_{ddd}). There are 32 formula-mass units per unit cell (z=32) and therefore 56 atoms in a primitive cell: 8 M^{II}, 16 Ga, 32 S. According to our XRD data and [1,9] the M^{II} atoms occupy square anti-prismatic sites formed by eight sulphur atoms (fig.2) (symmetry group: D_{4d}).

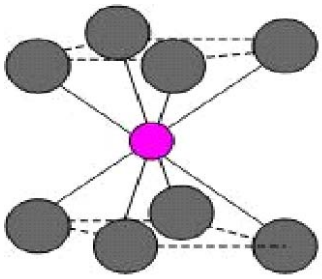

Fig.2. Schematic illustration of the local environment around one of the Ca ions in $CaGa_2S_4$ phosphors. The Ca ion occupies square antiprismatic sites (eightfold coordinated surrounded by S^{2-} ions).

Gallium atoms are tetrahedrally coordinated to four sulphur or atoms forming GaS_4 units (symmetry group: T_d) and the sulphur atoms are at the centre of deformed $M^{II}{}_2Ga_2$ tetrahedrons forming $SM^{II}{}_2Ga_2$ units.
The factor-group analysis [10] shows that vibration modes can be classified as Γ_v= 19 A_g + 21 B_{1g} + 22 B_{2g} + 22 B_{3g} +19 A_u + 20 B_{1u} + 21 B_{2u} + 21 B_{3u}. According to the symmetry rules, the A_g, B_{1g}, B_{2g} and B_{3g} modes are Raman active. Thus the factor group method predicts that the total number of Raman-active phonons is 84 for this structure. We observe the vibrations between Ga and S atoms but also those concerning the S neighbours of Ca or Ga atoms that move together along the anion-cation direction. The vibrations of S around Ca can be described in the CaS_8 molecular model: the Raman-active modes have the A_1, E_2 and E_3 symmetry in the D_{4d} group and their frequencies are independent of the Ca mass [11]. The vibrations of Ga-S bindings can be described in the GaS_4 molecular model in the Td symmetry.
The fact that the Ca mass has very slight influence on the Raman spectrum excludes the possibility of the SGa_2Ca_2 vibrating units. The interpretation of the spectrum in terms of vibrations of isolated groups seems to provide an adequate first approximation because the binding energy of the Ga-S bonds is significantly higher than that of the Ca-S bonds in $CaGa_2S_4$ compound. Thus the GaS_4 model seems to be more adequate than the CaS_8 model to interpret the $CaGa_2S_4$ Raman spectra. So we can formally consider the structure as consisting of isolated ions Ca and isolated GaS_4. The model of isolated vibrating GaS_4 and isolated Ca subunits is in good agreement with the fact that no mass effect of Ca atoms is observed.
We propose to investigate the Raman vibrations of Ga-S bindings in respect with Ga_2S_3 Raman spectrum because the vibrations of Ga_2S_3 have been also described in the GaS_4 molecular model in the T_d symmetry [12]. By analogy with the assignment of Ga_2S_3 vibrations, vibration lines of $CaGa_2S_4$ compound above 270 cm^{-1} are assigned to internal vibration modes due to stretching vibrations of S-S and Ga-S in the tetrahedral GaS_4 units. Among those located at frequencies lower than 200 cm^{-1} some may be due to bending vibrations of the GaS_4 tetrahedral units and others may correspond to external vibration modes issued from translation vibrations of molecular subunits (lattice modes)[13,14].

3.2 Luminescent properties

Fig. 3a and 3b show the excitation and emission spectra of the Tb^{3+} ion incorporated in $CaGa_2S_4$. In addition to the band below 290 nm which corresponds to an excitation via the host lattice, excitation specter contains an intense band.

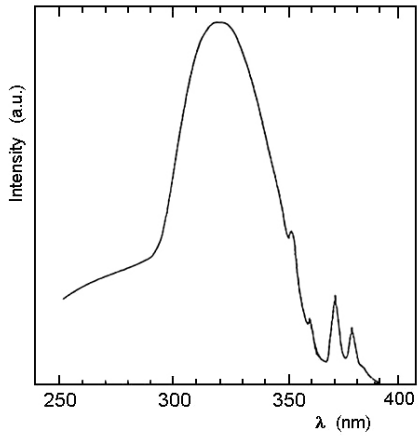

Fig.3a. Excitation spectra of $CaGa_2S_4$:Tb^{3+} at 300 K.(Excitation of the $^5D_4 \rightarrow {}^7F_5$ emission lines.)

For excitation into this band $CaGa_2S_4$:Tb^{3+} shows an intense visible emission at 300K. The probability of non-radiative transitions between $4f^n$ levels is dropped owing to the low phonon energies. Because of the large energy gap between the $^5D_4$ and $^7F_0$

(see fig.4) levels of Tb^{3+}, multiphonon de-excitation processes from the $^5D_4$ level are negligible. The most intense radiative transition originating this level, $^5D_4 \rightarrow {}^7F_5$, lies in the green, but because of the transitions to the other components ($^5D_4 \rightarrow {}^7F_6$, $^5D_4 \rightarrow {}^7F_4$, $^5D_4 \rightarrow {}^7F_3$) of the ^7F_J multiplet, the color purity (x=0.372, y=0.524, fig.7) is unsatisfactory.

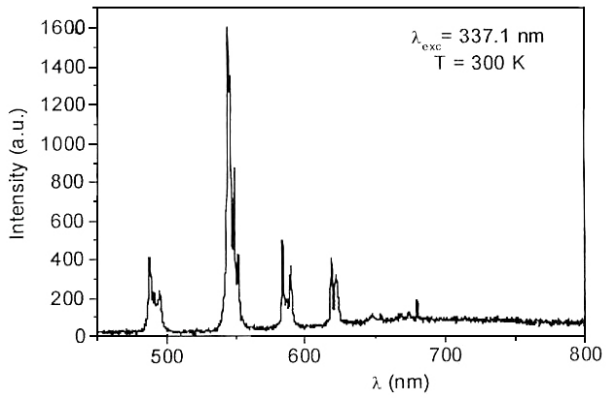

Fig.3b. Emission spectrum of the $CaGa_2S_4:Tb^{3+}$ at 300 K. (Excitation in the f→d band; $\lambda_{exc.}$=337.1 nm.)

However the lowest-energy f-d transitions of the latter are spin forbidden, so the first intense bands Tb^{3+} ion lie at close wave-lengths. The charge transfer and f-d bands lie at energies higher than that of the absorption edge of the host lattices. Among the non-radiative transition mechanisms leading to a thermal relaxation of the luminescent center a multiphonon process is often observed between 4f excited levels of rare-earth ions.

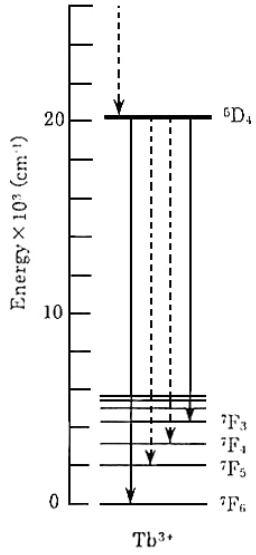

Fig.4. Diagram of energy transfer Tb^{3+} ion.

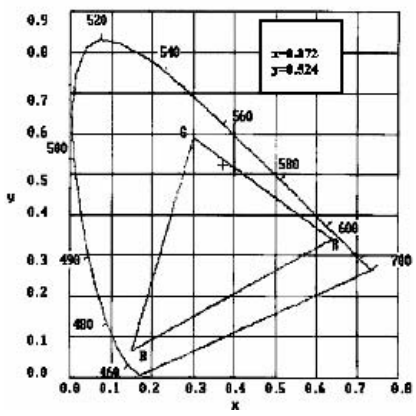

Fig.5. Color coordinates for $CaGa_2S_4:Tb^{3+}$ crystal. (R, G, B: CRT coordinates).

The non-radiative multiphonon transition probability is dependent on the energy difference between the electronic states ΔE and n, the number of phonons necessary to fill the energy gap, i.e. $\Delta E = n\hbar\omega$.

3.3. Decays

As all the main transitions observed come from the same $^5D_4$ excited level, we analyzed only the decay for the most intense transition ($^5D_4 \rightarrow {}^7F_5$) at 545 nm.

The fig.6a represents the fast decay at λ_{anal} = 545 nm. This fast decay must come from the broad band observed on the emission spectrum under λ_{exc} = 337.1 nm (Fig.3b).

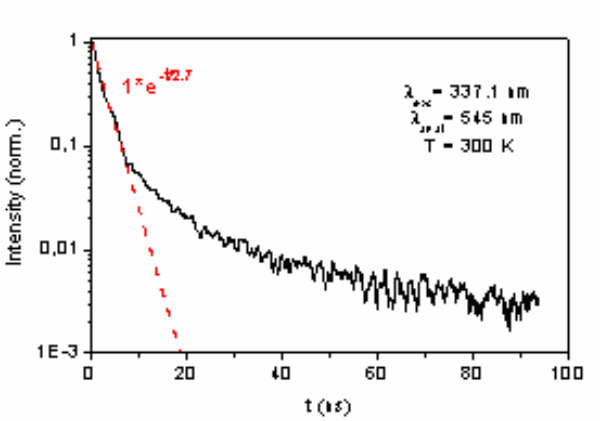

Fig 6a. Decay curve under λ_{exc}= 337.1 nm. The dashed line represents the decay time of 2.7 ns

The fig.6b represents the long decay at λ_{anal} = 545 nm. We made a fitting of the exponential part of this decay with a lifetime of 615 µs (fig.6b). This exponential part of 615 µs corresponds to the intrinsic lifetime of Tb^{3+}. At short time, the decay presents a non exponential part due to an energy transfer mechanism with nonradiative transitions and a loss of energy.

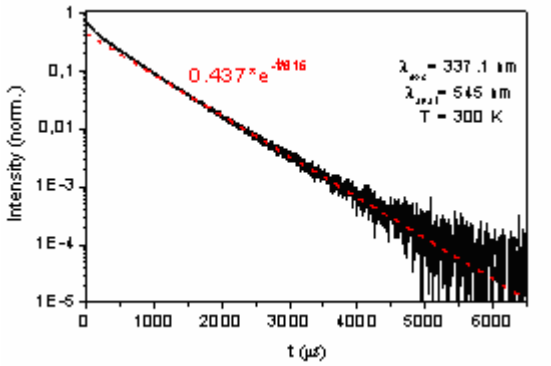

Fig.6b. Decay curve under λ_{exc}= 337.1 nm. The dashed curve represents the simulation of two exponential decays of 615 µs and 271 µs.

4. Conclusion

The Raman study of polycrystalline $CaGa_2S_4:Tb^{3+}$ compounds was performed to clarify the origins of the Raman vibrations. We observe that no vibration involving directly the divalent cation Ca is present in the Raman spectra since the mass of the Ca has very little influence on the vibration frequencies. The Raman vibrations depend essentially on the M^{II} cation size. Since the effect of the M^{II} cation on the $M^{II}Ga_2S_4$ Raman spectra is very slight we conclude that the orthorhombic thiogallates present nearly the same phonon energies whatever the M^{II} cation**..**

The non-radiative multiphonon transition probability is given by:

$$W_{NR}(\Delta E) = W_{NR}(0)\exp(-\alpha\Delta E/\hbar\omega).$$

The non-radiative multiphonon transition probability is increasing with the frequency increase of the high-energy phonons of the lattice [15]. In the case of EL materials, the energy exchange between electron and phonon is described by the electron-phonon interaction Hamiltonian. Under high electric field the most frequent scattering event is the emission of optical phonons and the energy relaxation of electrons is dominated by the coupling to the high-frequency modes. Scattering rate is lower for EL phosphor lattice presenting low high-frequency phonons [15]. For CL materials the rate of phonon energy loss is controlled by the highest energy phonons and the CL efficiency of the phosphors decreases with increasing phonon energy [16].Several conclusions can be drawn from Raman vibration spectra of $CaGa_2S_4$ compound. The optical high-frequency phonons of crystal we have to consider correspond to the vibration modes dominating the high-frequency domain, i.e. at about 35 and 45 meV.

References

[1] T.E.Peters and J.A.Baglio, J. Electrochem. Soc., 119, p. 230 (1972).
[2] P.C.Donohue and J.E.Hanlon, J.Electrochem.Soc., 121, p.137 (1974).
[3] W.A.Barrow, R.C.Coovert, E.Dickey, C.N.King, C.Laakso, S.S.Sun, R.T.Tuenge, R.Wentross, J. Kane, SID , p.761 (1993).
[4] A.N. Georgobiani, B.G.Tagiev, O.B.Tagiev, B.M. Izzatov, R.B. Jabbarov, Cryst. Res.Technol., 31, S 849-852 (1996).
[5] S.Iida, T.Matsumoto, N.Mamedov, G. An, Y. Maruyama, A. Bairamov, B. Tagiev, O.Tagiev, R. Jabbarov, Jpn.J.Appl.Phys. Vol.36, pp.L857-L859 (1997).
[6] Benalloul P., Barthou C. and Benoit J., J. of Alloys and Compounds, 275-277, p.709 (1998).
[7] I.Ronot-Limousin, A.Garcia, C.Foussier, C.Barthou, P.Benalloul and J.Benoit, J.Electrochem. Soc., 144, p.687 (1997)
[8] Robbins D J 1980 *J. Electrochem. Soc.* **127** 2694
[9] B.Eisenmann, M.Jakowski, W.Klee, H.Schafer, Revue de Chimie Minerale 20, 255 (1983).
[10] R.S.Halford, Journal of Chemical Physics, 14 (1), p.8 (1946).
[11] H.L.Schlafer and H.F.Wasgesstian, Theoret. Chim.Acta 1 369 (1963).
[12] G. Lucazeau and J.Leroy, Spectrochimica acta, 34A, p.29 (1978).
[13] N.N.Syrbu, V.E.L'vin, I.B.Zadnipru, V.M.Golovei, Sov.Phys.Semicond., 25(10), p.255 (1983).
[14] S.Barnier, M.Guittard and J.Flahaut, Mat. Res. Bull., 15, p.689 (1980).
[15] Phosphor Handbook, CRC press (1999).
[16] D.J.Robbins , J. Electrochem. Soc., 127, p.2694 (1980).